Dimensional change behavior of porous MgTi2O5 in reactive sintering

doi: 10.1016/j.ceramint.2017.01.079

Ceramics International
November 9, 2016

Dimensional change behavior of porous $MgTi_2O_5$ in reactive sintering

Yuta NAKAGOSHI[a], Yoshikazu SUZUKI[a,b*]

[a] Graduate School of Pure and Applied Sciences, University of Tsukuba, 1-1-1 Tennodai, Tsukuba, Ibaraki, 305-8573, Japan
[b] Faculty of Pure and Applied Sciences, University of Tsukuba, 1-1-1 Tennodai, Tsukuba, Ibaraki, 305-8573, Japan

Abstract

Volume-shrinkage of a sample in reactive sintering generally tends to be larger than that in conventional sintering. New techniques to suppress the volume shrinkage are eagerly needed for actual manufacturing. Recently, we have reported that reactively sintered porous $MgTi_2O_5$ from hydromagnesite and TiO_2 rutile showed less volume shrinkage than that from hydromagnesite and TiO_2 anatase. The result demonstrated that the compositional control of starting polymorphs can be a potential technique to optimize the volume shrinkage. In this paper, in order to evolve the reactive sintering technique, volume-changes during reactive sintering were dynamically monitored by thermomechanical analysis (TMA). The dimensional change behavior measured by TMA was linked up with the reaction behavior clarified by high-temperature X-ray diffraction (HT-XRD). In dilatometry curves, transient volume expansions were observed and they were well-explained by the formation and crystal growth of intermediate $MgTiO_3$ and objective $MgTi_2O_5$ particles.

Keywords:

A. Powders: solid state reaction; A. Sintering; B. Porosity; C: Thermal expansion; $MgTi_2O_5$; Reactive sintering

1. Introduction

Porous ceramics are light, chemically stable and highly thermal resistant, which have been widespread in aerospace, energy and environment fields as a light-weight high-temperature structural material. In the environmental field, diesel particulate filters (DPFs) and honeycombs carriers for automobiles were prime examples. Orthorhombic pseudobrookite-type ceramics generally have relatively low bulk thermal expansion [1-3]; the pseudobrookite-type crystal

* Corresponding author:
Division of Materials Science, Faculty of Pure and Applied Sciences,
University of Tsukuba, Ibaraki 305-8573, Japan
E-mail: suzuki@ims.tsukuba.ac.jp (Y. Suzuki)

structure has anisotropic thermal expansion, which induces inter- and intragranular microcracks in bulk polycrystals, resulting low bulk thermal expansion. Aluminum titanate (Al_2TiO_5) has been eagerly studied among pseudobrookite-type ceramics due to its low bulk thermal expansion. However, Al_2TiO_5 is metastable below 1200°C, so that Al_2TiO_5 tends to decompose into Al_2O_3 and TiO_2 rutile [4]. As an alternative pseudobrookite-type compound, we have focused on magnesium dititanate ($MgTi_2O_5$) as a light-weight high-temperature structural material due to its thermal stability below 1600°C [5-8].

Reactive sintering is an environmentally and economically friendly process because synthesis and sintering are carried out in one-step heating process. Therefore, reactive sintering can reduce some of the production costs [9-11]. Suzuki *et al.* reported the reactive sintering of porous $MgTi_2O_5$ from hydromagnesite ($Mg_5(CO_3)_4(OH)_2{\cdot}4H_2O$) and TiO_2 anatase mixture with LiF additive, where decomposed gasses from raw powders formed uniformly 3D network structure without using any pore-forming agent [12-14]. In the reactive sintering, however, the volume-shrinkage of a sample tends to be larger than in conventional sintering because of the simultaneous synthesis and decomposition. Thus, new techniques to control the volume shrinkage are eagerly needed for actual manufacturing.

As for the conventional sintering (*i.e.*, synthesis and sintering processes are separately conducted), sintering temperature is a key parameter and is flexible to control the volume shrinkage. On the other hand, as for the reactive sintering, sintering temperature is restricted by expected reactions. Therefore, besides changing the sintering temperature, alternative techniques to control the volume-shrinkage are strongly desired to popularize the reactive sintering. Recently, we have reported that reactively sintered porous $MgTi_2O_5$ from hydromagnesite and TiO_2 rutile showed less volume shrinkage than that from hydromagnesite and TiO_2 anatase [15]; the volume-shrinkage was well-controlled by changing TiO_2 anatase/rutile ratio, enabling even near-zero volume shrinkage [15]. This result has demonstrated that the compositional control of starting polymorphs can be a potential technique to optimize the volume shrinkage in reactive sintering.

In our last paper [15], volume-changes before/after reactive sintering were statically measured by geometrical dimensions of green and sintered samples. In this paper, in order to evolve the reactive sintering technique, volume-changes during reactive sintering were dynamically measured by thermomechanical analysis (TMA). The dimensional change behavior measured by TMA was linked up with the reaction behavior clarified by high-temperature X-ray diffraction (HT-XRD).

2. Experimental procedures

2.1 *In-situ* measurement for linear dimensional change behavior by TMA

Similarly to the previous paper [15], commercially available hydromagnesite ($Mg_5(CO_3)_4(OH)_2 \cdot 4H_2O$) powder, TiO_2 anatase powder (99% purity each, Kojundo Chemical Laboratory Co. Ltd.) and TiO_2 rutile powder (99.9% purity each, Kojundo Chemical Laboratory Co. Ltd.) were used as the starting materials. In this experiment, the following TiO_2 anatase/rutile compositions (in mole fraction) were used: (a) anatase : rutile = 100 : 0, (b) 75 : 25, (c) 50 : 50, (d) 25 : 75 and (e) 0 : 100. LiF powder (98.0%, Wako Pure Chemical, Osaka, Japan) was used as a mineralizer. Prior to the weighing, TG-DTA analysis (up to 1000°C) on each starting powder was conducted to determine the weight-loss during the heating. With the compositional calibration using TG-DTA results, hydromagnesite and TiO_2 powders (Mg:Ti = 1:2 in mole fraction) with LiF (0.5 wt.% for total starting powders) were wet-ball milled in ethanol for 24 h. The mixed slurries were vacuum dried, and the dried powders were put into the oven at 80°C overnight. The mixed powders, with a variety of TiO_2 anatase/rutile compositions (a)-(e), were then sieved through a 150-mesh screen (<100 μm).

The five mixed powders (2.0 g each) were uniaxially pressed into rectangular bars at 26.2 MPa for 1 min, re-pressed at the same conditions (except 90° rotation around pressing axis), and finally cold-isostatically pressed at 200 MPa for 10 min to obtain homogeneous green bars. The green rectangular bars were shaped into the dimensions of 19.8±0.05 mm × 3.9±0.05 mm × 5.3±0.05 mm by gentle grinding with abrasive paper. The linear dimensional change in length-direction of the green rectangular bars was measured by dilatometry with TMA (Thermo plus EVO, Rigaku, Tokyo, Japan). The samples were heated from ~25°C (R.T.) to 1100°C (ramp rate: 5°C/min), kept at 1100°C for 2 h, and cooled down to 30°C (5°C/min).

3. Result

3.1 *In-situ* measurement for dilatometry curves by TMA

Figure 1 shows the dilatometry curves in reactive sintering of five samples with various TiO_2 anatase/rutile compositions. The five solid lines demonstrate the dilatometry (left axis), and the broken line demonstrates the measurement temperature (right axis). The horizontal axis represents the elapsed time since the measurement started. All samples demonstrated complex dilatometry curves, which can be classified into five steps (Fig. 1).

STEP(i) (R.T. - 600°C)

In step(i), all dilatometry curves stepwise decreased. These stepwise changes can be attributed to the multistep decomposition of hydromagnesite, which was confirmed by HT-XRD analysis in our previous study (Fig. S1 [15]). Figure 2 shows the dilatometry curve in step(i) and TG curve of the sample(a) (TiO_2 anatase/rutile = 100/0 in the starting powder). The multistep mass change in step(i) was caused by the decomposition of hydromagnesite (Fig. S2). Hence,

the dimensional changes in step(i) was mainly governed by the decomposition of hydromagnesite.

STEP(ii) (600°C - 900°C)

In step(ii), all dilatometry curves had first expansion peaks. From the HT-XRD analysis (Fig. S1 [15]), $MgTiO_3$, an intermediate phase of MgO-TiO_2 system, is synthesized at this temperature range (600~900°C). Hence, these first expansion peaks appeared due to the formation and particle growth of $MgTiO_3$. With increasing rutile composition, the expansion peaks appeared at higher temperatures (Fig. 3(a)). This result indicated that $MgTiO_3$ particles were synthesized at higher temperature due to the less reactivity of TiO_2 rutile (*i.e.* the better reactivity of TiO_2 anatase). Because $MgTiO_3$ had already synthesized at ~600°C by using TiO_2 anatase, the dimensional changes of the samples using TiO_2 anatase were smaller than TiO_2 rutile in step(i). After the dilatometry peak in 600~900°C, the dilatometry curves decreased due to sintering.

STEP(iii) (900°C - 1100°C)

In step(iii), all dilatometry curves had second expansion peaks. From the HT-XRD analysis (Fig. S1 [15]), $MgTi_2O_5$ (the target phase) is synthesized at this temperature range (900~1100°C). Hence, these second expansion peaks appeared due to the formation and particle growth of $MgTi_2O_5$. Similarly to STEP(ii), these expansion peaks appeared at higher temperatures with increasing the rutile composition (Fig. 3(b)). This result also indicated that $MgTi_2O_5$ particles were synthesized at higher temperature due to less reactivity of TiO_2 rutile (*i.e.* better reactivity of TiO_2 anatase).

STEP(iv) (1100°C for 2h)

In step(iv), all dilatometry curves decreased due to the progress of sintering. Because $MgTi_2O_5$ particles from TiO_2 anatase source were easily sintered, the dimensional change with sintering became larger with increasing starting anatase composition.

STEP(v) (1100°C – 30°C)

In step(iv), the decrease of dilatometry curves stopped as soon as a cooling began. After that, dilatometry curves became almost constant because of the low bulk thermal expansion nature of pseudobrookite-type ceramics.

4. Discussion

4.1 Mechanisms of dimensional-change in reactive sintering of porous $MgTi_2O_5$

Analysis of dilatometry curves by TMA has been used to understand the sintering behavior, *e.g.*, the reactive sintering behavior of bauxite (yielding kaolinite–corundum composite) by Djangang et al. [16]. In the reference [16], during the heating, thermal decomposition of hydroxide and phase transformations from metastable to stable phases tended to promote the volume-shrinkage. In this study, the dilatometry curves actually decreased with the decomposition of hydromagnesite in step(i). However, we observed the size expansions in step(ii) and step(iii), corresponding to the formation of $MgTiO_3$ and $MgTi_2O_5$. These dimensional increases were probably caused by the particle growth, the neck growth and the 3-D framework formation.

To confirm the reason of the size expansions, we observed the microstructures at intermediate temperatures for the sample of (a) TiO_2 anatase/rutile = 100/0 (Fig. 4). In the green compact, somewhat large plate-like particles were hydromagnesite and fine spherical particles were TiO_2 anatase (see photos of raw powders, Fig. S3). For step(i) at 540°C, the fine MgO particles decomposed from hydromagnesite coexisted with the TiO_2 anatase particles. Some undecomposed hydromagnesite were still observed. For step(ii) at 770°C, spherical particles were TiO_2 anatase and $MgTiO_3$, judged from XRD. Compared with green compact and step(i), step(ii) showed somewhat larger particles and porous structure. By building up this 3-D porous structure, the linear dimension presumably increased in step(ii). For step(iii) at 1000°C, 3-D porous structure of semi-equiaxed $MgTi_2O_5$ particles was confirmed. After the measurement, $MgTi_2O_5$ particles grew into rod-like particles due to pseudobrookite-type structure with strong anisotropic crystal growth. Figure 5 schematically explains the apparent volume-change and microstructural evolution.

In our previous report [15], we set up a hypothesis for volume-change behavior in reactive sintering of porous $MgTi_2O_5$ from hydromagnesite and TiO_2 mixture, where the samples first expanded due to the H_2O and CO_2 gas emissions by the decomposition of hydromagnesite, and then they shrank by the progress of sintering. Throughout this research, the expansion at step(ii) and step(iii) can be rather attributed to the formation and growth of $MgTiO_3$ and $MgTi_2O_5$ particles, respectively.

4.2 Dimensional change in three directions

In this study, the dimensional-changes in only one axis were *in-situ* monitored. To discuss the dimensional change behavior for whole rectangular samples, it seems to be necessary to measure the dimensional-change in three axes. However, the dimensional changes before and after TMA measurements of thee-axes were almost same in each sample (Table 1). Hence, the dimensional changes in one axis can be regarded as the dimensional changes in all direction.

4.3 Improvement of the sintering program

In-situ dimensional change measurement can help to determine the suitable sintering program. Although controlling the dimensional change (ΔL [mm]) before and after sintering is important, controlling the speed of relative dimensional change ($(\Delta L/L)/\Delta t$ [%/min]) is also important for the prevention of cracks and deformation. By differentiation of the relative dimensional change ($\Delta L/L$ [%]) with respect to time (Δt [min]), the relative dimensional change speed ($(\Delta L/L)/\Delta t$ [%/min]) can be evaluated. Figure 6 represents the relative dimensional change speed (DTMA) of the sample (e) (anatase/rutile = 0/100). The rapid dimensional change can be suppressed by slowing down the ramp rate or by adding the holding steps at around 410°C, 770°C and 1000°C. Therefore, an improved heating program (Table 2) was proposed. *In-situ* dimensional change measurement of the sample (e) was carried out with improved heating program. Figure 7 shows the results of relative dimensional change speed (DTMA) by using (a) original program and (b) improved program. In Fig. 7(b), sharp DTMA peaks around 410°C, 770°C and 1000°C almost disappeared. It is worthy of note that the dimensional changes by improved program became identical for all three axes, which enables ideal homogeneous shrinkage during reactive sintering (Table 3). In addition, the relative dimensional change speed was successfully controlled without changing volume-change by improving the sintering program.

4. Conclusion

In this paper, the dimensional change behavior in reactive sintering of porous $MgTi_2O_5$ was *in situ* analyzed by using TMA by linking up with HT-XRD analysis. The transient volume expansions were observed and these phenomena were well-explained by the formation and crystal growth of $MgTiO_3$ and $MgTi_2O_5$ particles, which resulted in 3-D framework structure. *In-situ* dimensional change measurement was really effective to improve the sintering program. It is worthy of note that the dimensional changes by improved program became identical for all three axes, which enables ideal homogeneous shrinkage during reactive sintering. We believe the *in-situ* dimensional-change measurement can be a powerful tool to improve the reactive sintering.

Acknowledgment

We thank Prof. Tamotsu Koyano at Cryogenics Division, Research Facility Center, University of Tsukuba for his help on SEM observation.

References

[1] G. Bayer, Thermal expansion characteristics and stability of pseudobrookite-type compounds, Me_3O_5, J. Less-Common. Metal. 24 (1971) 129-138.

[2] J. J. Cleveland, R. C. Bradt, Grain size/microcracking relations for pseudobrookite oxides, J. Am. Ceram. Soc. (1978) 478-481.

[3] D. Taylor, Thermal expansion data: XI. complex oxides, A_2BO_5, and the garnets, Br. Ceram. Trans. J. 86 (1987) 1-6.

[4] E. Kato, K. Daimon. J. Takahashi, Decomposition temperature of β-Al_2TiO_5, J. Am. Ceram. Soc. 63 (1980) 355-356.

[5] I. Shindo, Determination of the phase diagram by the slow cooling float zone method: the system MgO-TiO_2, J. Cryst. Growth 50 (1980) 839-851.

[6] J. Hauck, Crystallography and phase relations of MeO-M_2O_3-TiO_2 systems (Me = Fe, Mg, Ni; M = Al, Cr, Fe), J. Solid State Chem. 36 (1981) 52-65.

[7] B. A. Wechsler, A. Navrotsky, Thermodynamics and structural chemistry of compounds in the system MgO-TiO_2, J. Solid State Chem. 55 (1984) 165-180.

[8] B. A. Wechsler, R. B. von Dreele, Structure refinements of Mg_2TiO_4, $MgTiO_3$ and $MgTi_2O_5$ by time-of-flight neutron powder diffraction, Acta Cryst. B 45 (1989) 542-549.

[9] S. Zhu, S. Ding, H. Xi, Q. Li, R. Wang, Preparation and characterization of SiC/cordierite composite porous ceramics, Ceram. Int. 33 (2007) 115-118.

[10] S. Nikodemski, J. H. Tong, R. O'Hayre, Solid-state reactive sintering mechanism for proton conducting ceramics, Solid State Ionics. 253 (2013) 201-210.

[11] F. Wang, J. Ye, G. He, G. Liu, Z. Xie, J. Li, Preparation and characterization of porous $MgAl_2O_4$ spinel ceramic supports from bauxite and magnesite , Ceram. Int. 41 (2015) 7374-7380.

[12] Y. Suzuki, M. Morimoto, Porous $MgTi_2O_5$/$MgTiO_3$ composites with narrow pore-size distribution: *in situ* processing and pore structure analysis, J. Ceram. Soc. Jpn. 118 (2010) 819-822.

[13] Y. Suzuki, M. Morimoto, Uniformly porous $MgTi_2O_5$ with narrow pore-size distribution: *in situ* processing, microstructure and thermal expansion behavior, J. Ceram. Soc. Jpn. 118 (2010) 1212-1216.

[14] Y. Suzuki, T. S. Suzuki, Y. Shinoda, K. Yoshida, Uniformly porous $MgTi_2O_5$ with narrow pore-size distribution: XAFS study, improved *in situ* synthesis, and new *in situ* surface coating, Adv. Eng. Mater. 14 (2012) 1134-1138.

[15] Y. Nakagoshi, J. Sato, M. Morimoto, Y. Suzuki, Near-zero volume-shrinkage in reactive sintering of porous $MgTi_2O_5$ with pseudobrookite-type structure, Ceram. Int. 42 (2016) 9139-9144.

[16] C. N. Djangang, E. Kamseu, M. K. Ndikontar, G. L. L. Nana, J. Soro, U. C. Melo, A. Elimbi, P. Blanchart, D. Njopwouo, Sintering behaviour of porous ceramic kaolin–corundum composites: phase evolution and densification, Mater. Sci. Eng. A 528 (2011) 8311-8318.

Tables

Table 1 Dimensional change before and after the reactive sintering in three axes and standard deviation for them. L: Length. a: narrow side. b: long side.

Sample	Dimensional change [%]			standard
	⊿L/L	⊿a/a	⊿b/b	deviation
(a) A/R = 100/0	-8.2	-8.7	-8.4	0.21
(b) A/R = 75/25	-4.0	-3.9	-3.7	0.12
(c) A/R = 50/50	-0.8	-0.9	-1.0	0.08
(d) A/R = 25/75	1.2	1.3	1.5	0.12
(e) A/R = 0/100	2.3	2.7	2.6	0.16

Table 2 Original heating program and improved heating program.

Original heating program	heating: R.T.- 1100°C (5 °C/min)
	holding: 1100°C (120 min)
	cooling: 1100°C-30°C (5 °C/min)
Improved heating program	heating: R.T.- 700°C (2 °C/min)
	holding: 700°C (60 min)
	heating: 700°C-950°C (2 °C/min)
	holding: 950°C (30 min)
	heating: 950°C-1100°C (2 °C/min)
	holding: 1100°C (120 min)
	cooling: 1100°C-30°C (5 °C/min)

Table 3 Dimensional change before and after reactive sintering in three axes-and volume change. L: Length. a: narrow side. b: long side.

Sample	⊿L/L [%]	⊿a/a [%]	⊿b/b [%]	⊿V/V [%]
(a) Original program	2.3	2.7	2.6	7.8
(b) Improved program	2.5	2.5	2.5	7.7

Figure captions

Fig. 1 Dilatometry curves (solid lines) during reactive sintering of five samples with various TiO_2 anatase/rutile compositions: (a) anatase/rutile = 100/0, (b) 75/25, (c) 50/50, (d) 25/75, (e) 0/100. The broken line demonstrates measurement temperature.

Fig. 2 Comparison of the dilatometry curve in step(i) in Fig. 1 and the TG curve of the sample (a) (TiO_2 anatase/rutile = 100/0 in starting powder). The dilatometry curve decreased in three steps associated with decomposition of hydromagnesite.

Fig. 3 Temperature of peaks for dilatometry curves in Fig. 1: (a) in step(ii), (b) in step(iii). With increasing TiO_2 rutile composition in starting powders, the temperatures of peaks became higher.

Fig. 4 Microstructural change during the reactive sintering. TMA measurement was stopped at the points (1)-(5) in the graph, and then, microstructures were observed by SEM. TiO_2 anatase/rutile composition of starting powder was 100/0.

Fig. 5 Schematic illustration for the apparent volume-change behavior and microstructural evolution of porous $MgTi_2O_5$ from hydromagnesite and TiO_2.

Fig. 6 Relative dimensional change speed (DTMA) for the sample (e) (TiO_2 anatase/rutile = 0/100 in the starting powder). The DTMA sharply decreased around 410°C, and increased around 770°C and 1000°C.

Fig. 7 Relative dimensional change speed (DTMA) for the sample (e) (TiO_2 anatase/rutile = 0/100 in the starting powder): (a) original program as in Fig. 6 and (b) improved program.

Figures

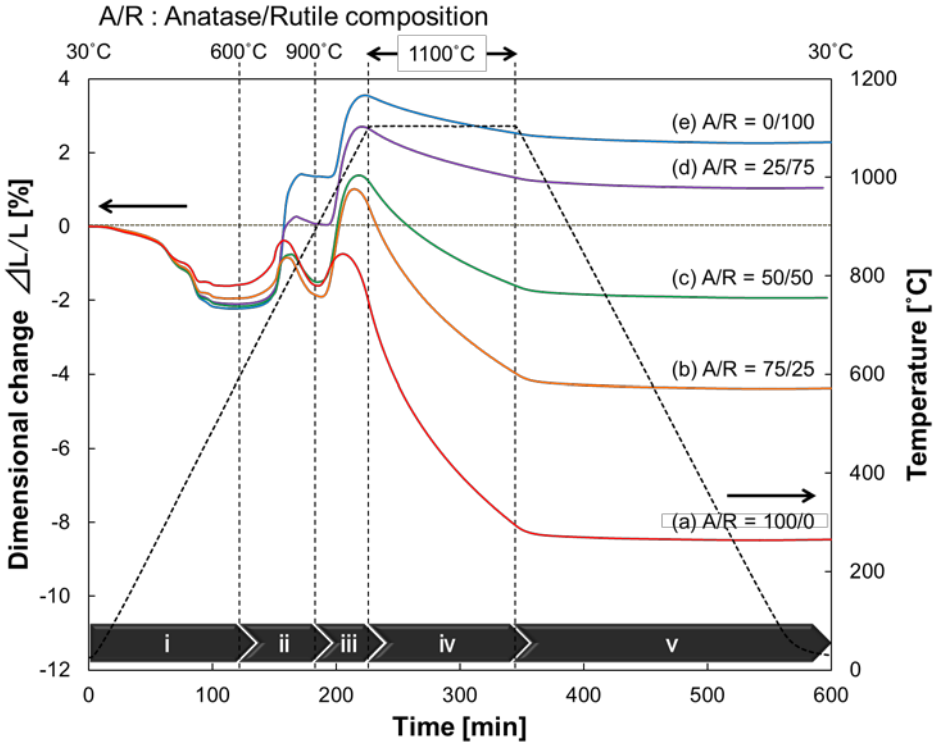

Fig. 1 Dilatometry curves (solid lines) during reactive sintering of five samples with various TiO_2 anatase/rutile compositions: (a) anatase/rutile = 100/0, (b) 75/25, (c) 50/50, (d) 25/75, (e) 0/100. The broken line demonstrates measurement temperature.

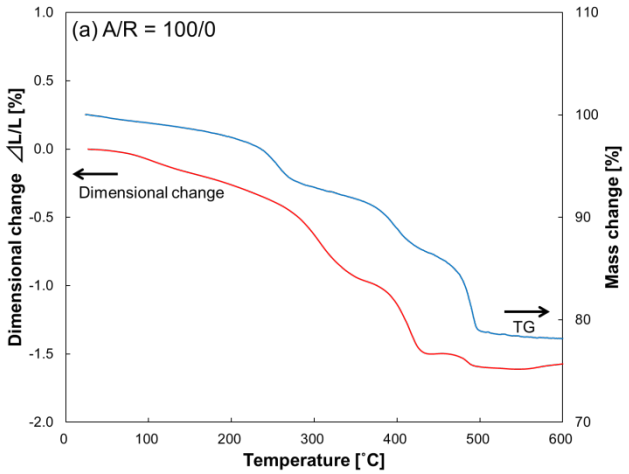

Fig. 2 Comparison of the dilatometry curve in step(i) in Fig. 1 and the TG curve of the sample (a) (TiO_2 anatase/rutile = 100/0 in starting powder). The dilatometry curve decreased in three steps associated with decomposition of hydromagnesite.

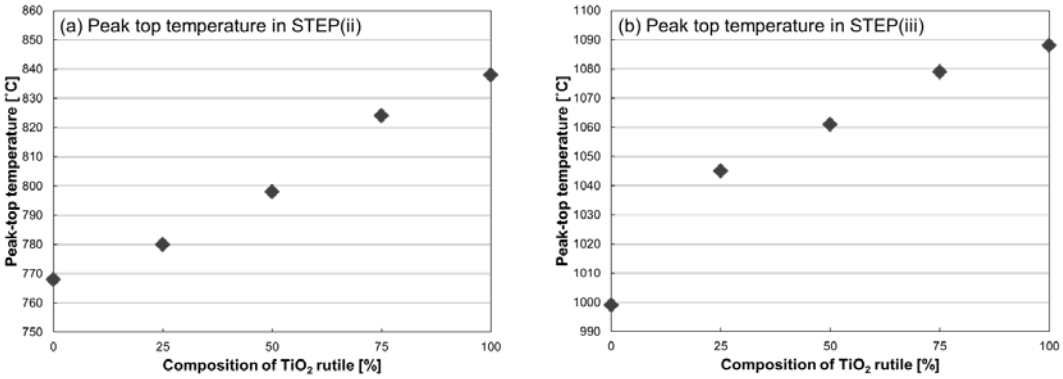

Fig. 3 Temperature of peaks for dilatometry curves in Fig. 1: (a) in step(ii), (b) in step(iii). With increasing TiO_2 rutile composition in starting powders, the temperatures of peaks became higher.

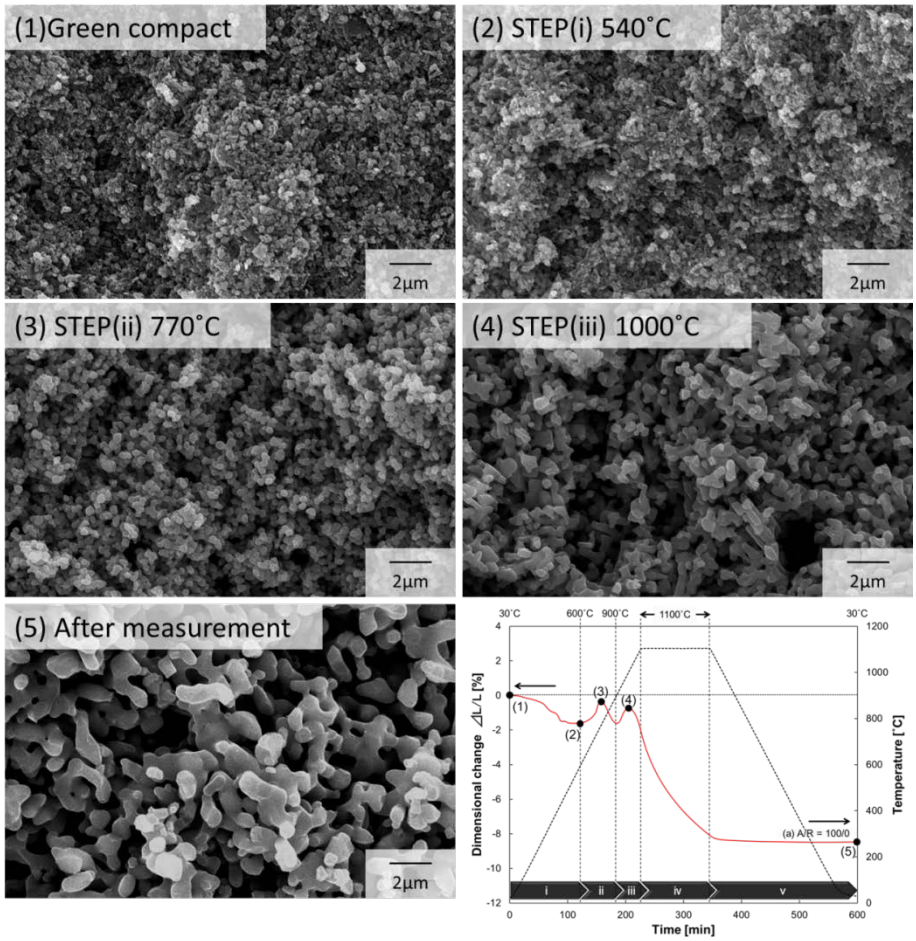

Fig. 4 Microstructural change during the reactive sintering. TMA measurement was stopped at the points (1)-(5) in the graph, and then, microstructures were observed by SEM. TiO_2 anatase/rutile composition of starting powder was 100/0.

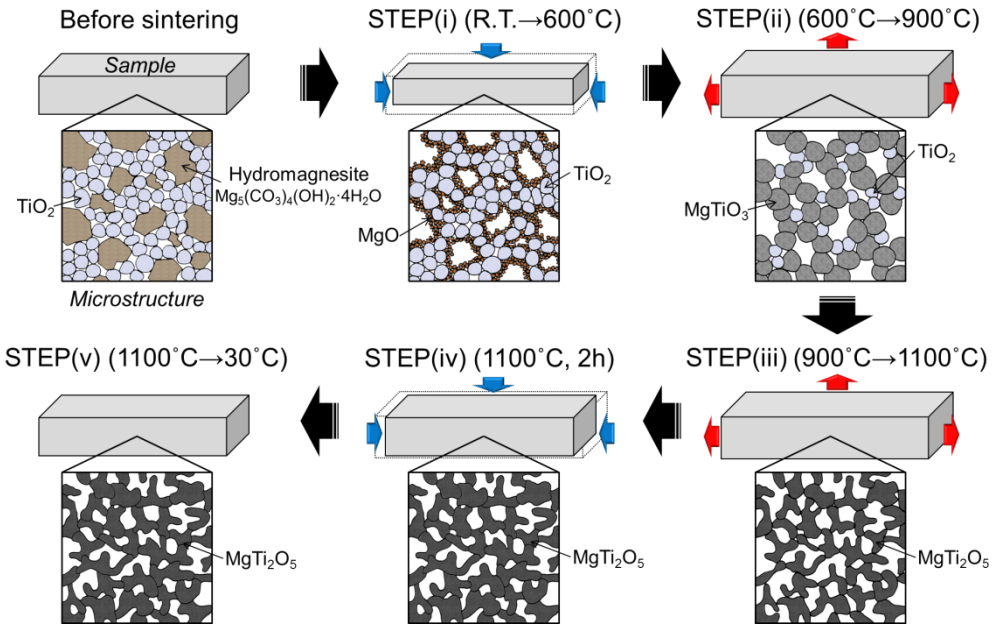

Fig. 5 Schematic illustration for the apparent volume-change behavior and microstructural evolution of porous $MgTi_2O_5$ from hydromagnesite and TiO_2.

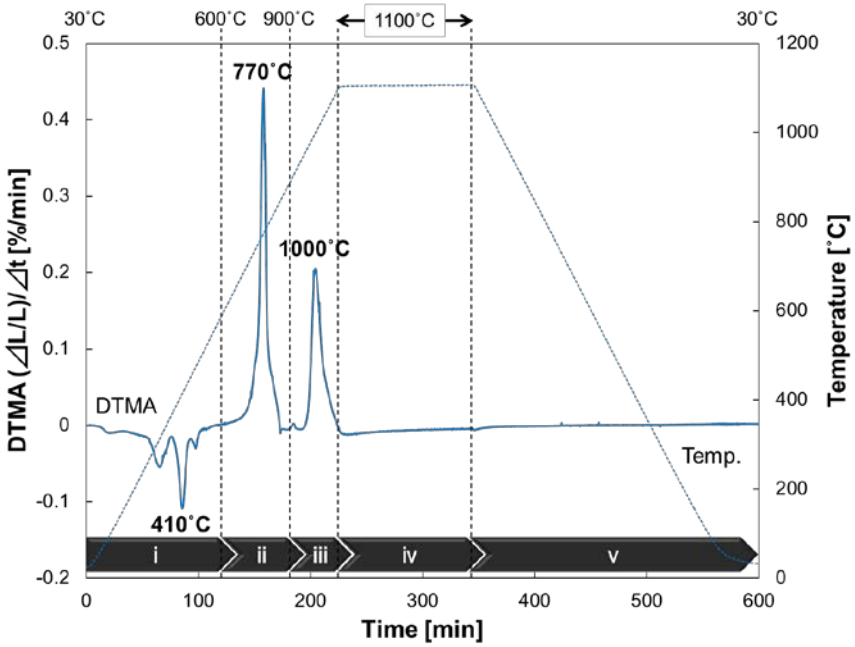

Fig. 6 Relative dimensional change speed (DTMA) for the sample (e) (TiO_2 anatase/rutile = 0/100 in the starting powder). The DTMA sharply decreased around 410°C, and increased around 770°C and 1000°C.

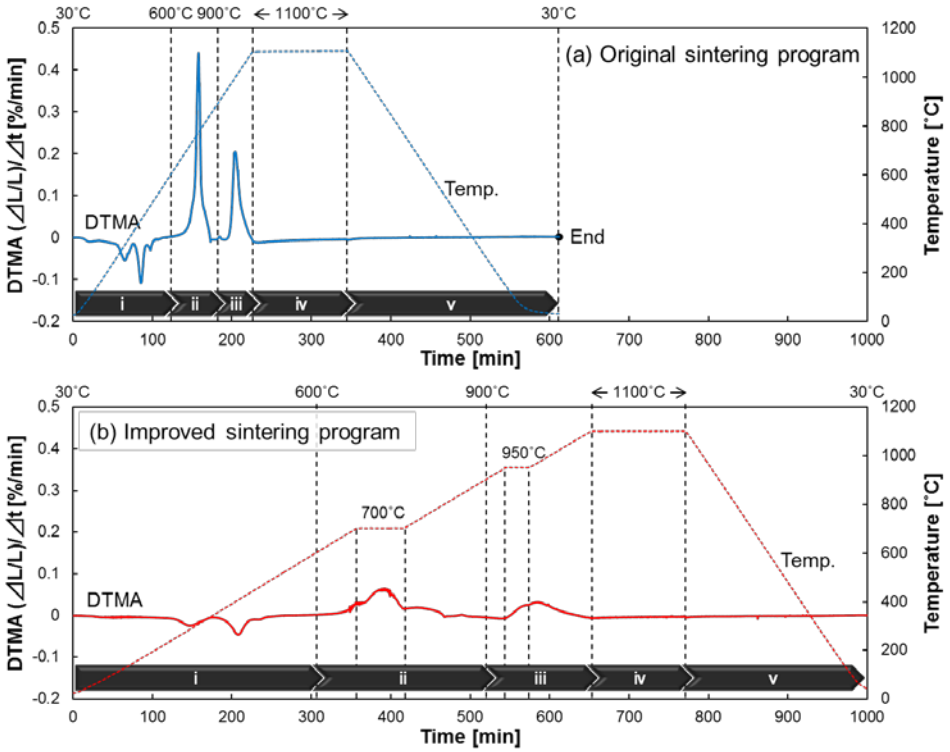

Fig. 7 Relative dimensional change speed (DTMA) for the sample (e) (TiO_2 anatase/rutile = 0/100 in the starting powder): (a) original program as in Fig. 6 and (b) improved program.

Supporting information

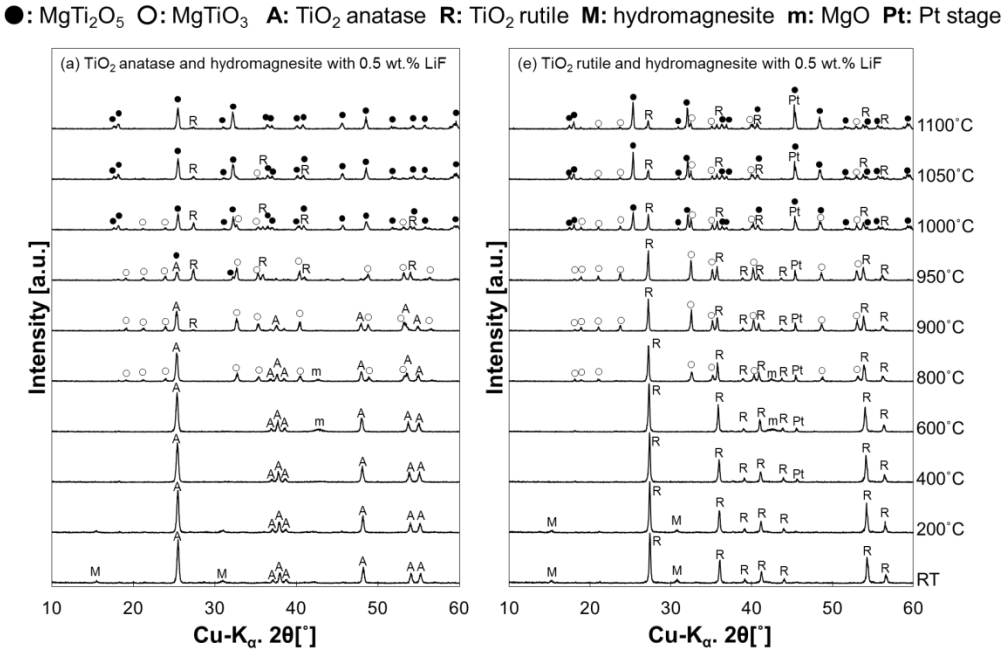

Fig. S1 High-temperature *in situ* XRD patterns for the selected mixed powders: (a) the hydromagnesite and TiO_2 anatase, and (e) the hydromagnesite and TiO_2 rutile mixed powder both with 0.5 wt.% LiF. Formation temperatures of $MgTiO_3$ and $MgTi_2O_5$ were almost the same in the both mixed powders. (*Ceram. Int.* **42** (2016) 9139-9144 [16], Copyright permission from Elsevier no. 3982940482091)

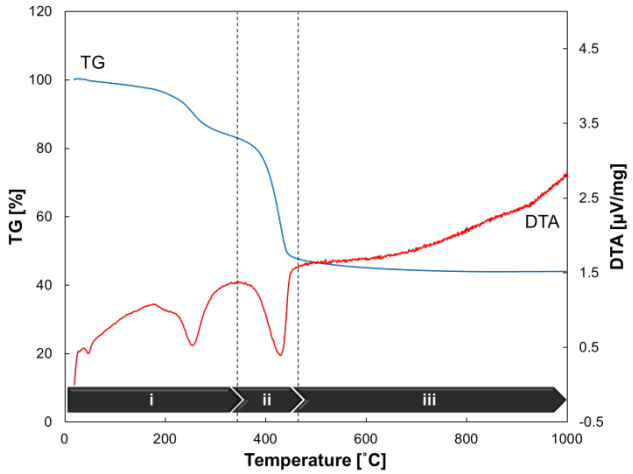

Fig. S2 TG-DTA curves (5°C/min) for the hydromagnesite powder used in this study. TG curve has three steps associated with decomposition.

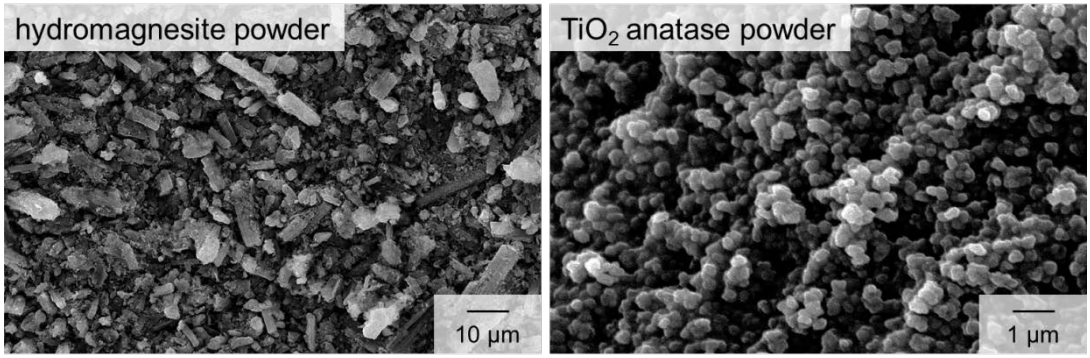

Fig. S3 SEM micrographs of raw hydromagnesite and TiO_2 anatase powders used in this study.

Appendix (LiF doping effect)

In order to clarify the effect of crystal growth on dimensional-change during the reactive sintering, mineralizer (LiF) doping effect was also studied by TMA; the dilatometry curves of the two-type of green bars (non-doped anatase-type and non-doped rutile-type) were also measured in the same manner as shown in the main text (Fig. S4).

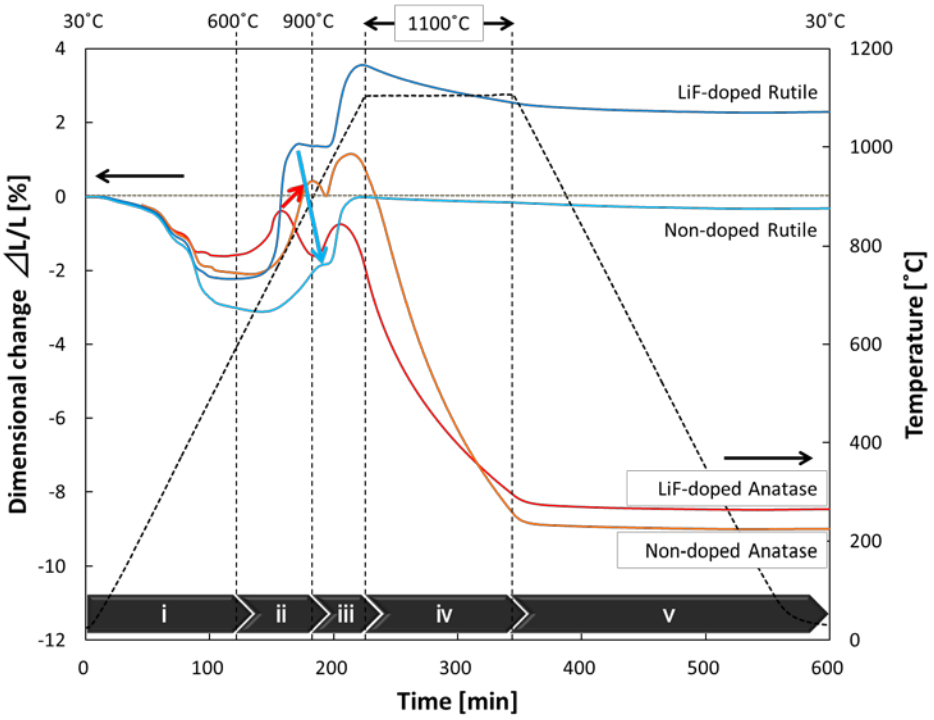

Fig. S4 Dilatometry curves in the reactive sintering of four samples using TiO_2 anatase or rutile with/without LiF.

Nevertheless with or without LiF, the dilatometry curves had five steps as same as Fig.1. However, for the samples without LiF doping, expansion peaks corresponding to the formations of $MgTiO_3$ clearly shifted to higher temperatures (red and blue arrows). This result suggested that LiF-doping accelerated the formation of $MgTiO_3$, and changed the 3-D framework formation. As can be seen in Fig. S5 (after TMA measurment), some elongated or irregular shape $MgTi_2O_5$ grains were finally formed for the LiF-doped samples, which resulted in the less shrinkage compared with non-doped samples.

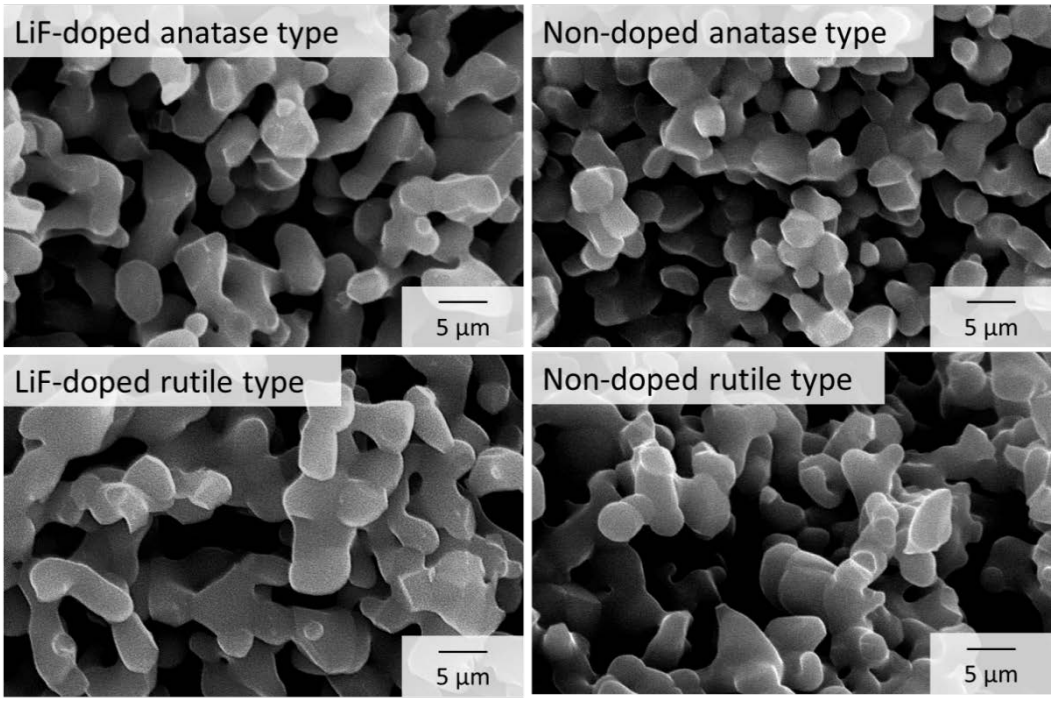

Fig. S5 SEM micrographs for TMA samples after measurement.